PIN-driven auxin transport emerged early in streptophyte evolution

Roman Skokan[1,2,8], Eva Medvecká[3,8], Tom Viaene[4], Stanislav Vosolsobě[1], Marta Zwiewka[3], Karel Müller[2], Petr Skůpa[2], Michal Karady[5], Yuzhou Zhang[6], Dorina P. Janacek[7], Ulrich Z. Hammes[7], Karin Ljung[5], Tomasz Nodzyński[3], Jan Petrášek[1,2] and Jiří Friml[6*]

[1] Department of Experimental Plant Biology, Faculty of Science, Charles University, 128 44 Prague 2, Czech Republic

[2] The Czech Academy of Sciences, Institute of Experimental Botany, 165 02 Praha 6, Czech Republic

[3] CEITEC - Central European Institute of Technology, Masaryk University, Mendel Centre for Genomics and Proteomics of Plants Systems, 625 00 Brno, Czech Republic

[4] Department of Plant Systems Biology, VIB, and Department of Plant Biotechnology and Bioinformatics, Ghent University, 9052 Gent, Belgium

[5] Department of Forest Genetics and Plant Physiology, Umeå Plant Science Centre, Swedish University of Agricultural Sciences, 901 83 Umeå, Sweden

[6] Institute of Science and Technology Austria (IST Austria), 3400 Klosterneuburg, Austria

[7] School of Life Sciences Weihenstephan, Technical University of Munich, 85354 Freising, Germany

[8] Co-first authors.

* Correspondence to: jiri.friml@ist.ac.at

Abstract

PIN-FORMED (PIN) transporters mediate directional, intercellular movement of the phytohormone auxin in land plants. To elucidate the evolutionary origins of this developmentally crucial mechanism, we analyzed the single PIN homolog of a simple green alga *Klebsormidium*. KfPIN functions as a plasma membrane localized auxin exporter in land plants and heterologous models. While its role in algae remains unclear, PIN-driven auxin export is likely an ancient and conserved trait within streptophytes.

Main text

Asymmetric distribution of the hormone auxin orchestrates many aspects of plant development. Auxin gradients are largely dependent on its directional (polar), cell-to-cell transport mediated by the asymmetrically distributed, plasma membrane (PM) localized PIN-FORMED (PIN) transmembrane auxin efflux transporters (Adamowski and Friml, 2015). PINs are omnipresent in the genomes of land plants (Bennett et al., 2015) and are functionally conserved between higher vascular land plants and bryophytes (Viaene et al., 2014). Land plants evolved from and are embedded in the "streptophyte" lineage together with freshwater green algae called "charophytes" (as further) (Leliaert et al., 2012). While charophyte full genome evidence is scarce, it is already clear they possess and express PIN homologs (Hori et al., 2014; Ju et al., 2015; Nishiyama et al., 2018). They produce the major native auxin indole-3-acetic acid (IAA) and some related compounds (Zizkova et al., 2017) and polar auxin transport was even shown in the morphologically very complex charophyte *Chara corallina* (Boot et al., 2012). However, charophytes are just beginning to emerge as model organisms and the function of their PIN-like proteins has yet been unaddressed. The charophyte genus *Klebsormidium* with filament-type multicellularity represents a sister lineage to the morphologically more complex streptophytes (Lelieart et al., 2012). *Klebsormidium nitens* has been the first charophyte alga to have its genome sequenced and contains a single PIN homolog (Hori et al., 2014), and at least one *(KfPIN)* is expressed in *Klebsormidium flaccidum* (Ju et al., 2015). The growth of *K. nitens* has been shown to respond to higher concentrations of exogenously applied auxins (Ohtaka et al., 2017). We decided to study the PIN/s of *Klebsormidium* species (particularly *Kf*PIN) to gain insight into the evolutionary origins of PIN family's role in auxin transport.

To address the properties of *Kf*PIN protein from *Klebsormidium*, where experimental options are limited, we used several land plant models well suited for studying auxin transport, i.e. the bryophyte *Physcomitrella patens*, the angiosperm *Arabidopsis thaliana* and the cell culture of *Nicotiana tabacum* cv. Bright-Yellow 2 (BY-2).

Stable expression of *Kf*PIN or of its translational fusion to green fluorescent protein (GFP) in *P. patens* under rice actin promoter (*pACT::KfPIN* or *pACT::KfPIN:GFP*) generated a phenotype similar

to one resulting from overexpressing its native or the *A. thaliana* PM-resident PIN proteins (Viaene et al., 2014) and indicative of auxin starvation, such as growth inhibition and reduced gametophore initiation in protonemal cultures (Fig. 1a-c). In *A. thaliana*, CaMV 35S promoter-mediated stable *Kf*PIN expression (*35S::KfPIN*) produced plants with impaired root gravitropism and abnormal leaf vasculature patterning (Fig. 1d-g), phenotypes related to defective PIN-driven auxin transport (Luschnig et al., 1998; Zhang et al., 2011; Xi et al, 2016). Finally, estradiol-induced *Kf*PIN expression in BY-2 cells (*XVE::KfPIN*) produced markedly elongated cells (Fig. 1h,i), a hallmark of auxin starvation following upregulation of characterized angiosperm PIN auxin exporters (Petrasek and Zazimalova, 2006). Hence, strong *Kf*PIN expression in all these plant models causes growth reactions indicative of distorted auxin homeostasis, likely via changes in cellular auxin transport.

Next, we tested for auxin transport capability of *Kf*PIN. The transgenic *pACT::KfPIN:GFP* protonemata of *P. patens* showed upregulated excretion of auxin into the culture medium (Fig. 2a). In *A. thaliana*, the PIN ectopic expression in root hairs is inverse proportional to their elongation (Ganguly et al., 2010) and the same effect was observed in *35S::KfPIN* lines (Fig. 2b,c). Both of these results are indicative for auxin export activity (Viaene et al., 2014). The most direct evidence comes from the accumulation and retention assays of ^{3}H-labeled auxins, where BY-2 cells (Petrasek and Zazimalova, 2006) and the oocytes of *Xenopus laevis* (Fastner et al., 2017) are well established models. When expression was induced in *XVE::KfPIN* BY-2 cells, these showed decreased accumulation of labelled auxins compared to non-induced controls (Fig. 2d,e). No differences were observed in the competition assay with non-labelled auxin precursor tryptophan or in the accumulation of inactive auxin analogue benzoic acid (Supplementary Fig. 1). Of note, the *Kf*PIN-mediated auxin efflux in BY-2 cells was less sensitive to inhibition by 1-N-Naphthylphthalamic acid (NPA) (Fig. 2d,e). In the non-plant frog model, plant PINs have been shown to export auxin when co-expressed with plant kinases such as PINOID (PID) (Zourelidou et al., 2014), and the same was observed for *Kf*PIN in this system (Fig 2f,g). These results strongly suggest a substrate-specific auxin transport function of the *Kf*PIN protein.

The above observations are consistent with *Kf*PIN auxin transport action at the PM, leading us to investigate its cellular localization pattern. The *pACT::KfPIN:GFP* transgenic protonemal filaments of

P. patens showed fluorescence at the PM, co-aligning with the marker dye FM 4-64 (Fig. 3a). The intracellular signal apparent in both red and green channels is a common autofluorescence in protonemal tissue and does not reflect the specific transgene fluorescence (Viaene et al., 2014). Unlike the native PM-localized *Pp*PINs (Viaene et al., 2014), *Kf*PIN was not localized polarly. The same fusion construct transformed into BY-2 cells under estradiol-inducible promoter (*XVE::KfPIN:GFP*) resulted upon induction in a PM-specific signal, co-aligning with FM4-64 staining, and a weaker ER signal likely resulting from the high expression rate (Fig. 3b). Importantly, the induced *XVE::KfPIN:GFP* BY-2 cells also showed increased ^{3}H-labeled auxin efflux and developed the elongated phenotype indicative of auxin starvation (Supplementary Fig. 1), correlating with the intensity of *Kf*PIN:GFP fluorescence within individual cells (Supplementary Fig. 2), which demonstrates functionality of the GFP-tagged version. Finally, *A. thaliana* plants transformed with *KfPIN:GFP* translational fusion expressed under the native *At*PIN2 promoter (*PIN2::KfPIN:GFP*) revealed a PM localization pattern in roots, which was apolar (Fig. 3c), unlike that of the native *At*PIN2 protein (Muller et al., 1998) and in line with the apolar *Kf*PIN:GFP pattern observed in *P. patens* protonema. These results show that *Kf*PIN expressed in land plant models localizes predominantly to the PM.

With the use of land plants we have obtained ample evidence into the auxin transport properties of *Kf*PIN. Therefore, we strove to obtain supporting evidence in *Klebsormidium*. RT-PCR revealed a stable transcription pattern of the *KfPIN* homolog in *K. nitens* throughout a subculture interval (Supplementary Fig. 3). To detect the native *Kf*PIN protein localization pattern, we performed immunostaining experiments, having designed an anti-*Kf*PIN specific antibody and adjusted the staining protocol (Paciorek et al., 2006) for the algal material. In the successfully stained cells, we observed a signal localized to the surface (Fig. 3d,e), whereas none was observed in control experiments without primary antibodies (Fig. 3f) or with primary antibodies against *A. thaliana* PIN1 and PIN2 (Supplementary Fig. 2). Immunostaining against α-tubulin served as a positive control (Supplementary Fig. 2). The same anti-*Kf*PIN antibody also produced a cell surface signal in the roots of *35S::KfPIN A. thaliana* plants, which was absent in wild type roots (Supplementary Fig. 2). As *Klebsormidium* is non-transformable, we attempted to bring direct evidence for auxin transport

between cells and environment in wild type alga by measuring the accumulation of ^{3}H-labeled auxins as in BY-2. These experiments were, however, technically non-feasible due to the likely prevalent IAA binding to the surface over entry into cells (Supplementary Fig. 3). However, in our investigation of the biosynthesis of auxin and its release into the culture medium throughout the subculture interval of *K. nitens,* we did detect IAA in both the biomass and culture medium, especially in the advanced stage of culture growth (Supplementary Fig. 4).

Using land plant models, we show that the PIN homolog of *Klebsormidium* is capable of a substrate-specific auxin transport action at the PM, which is typical for the so called 'canonical' PIN proteins of land plants (Petrasek et al., 2006). Unlike the canonical PINs, however, *Kf*PIN could not localize polarly, which is a crucial mechanism to restrict the direction of auxin flow (Adamowski and Friml, 2015). The native *Kf*PIN localization pattern we observed in *Klebsormidium* was peripheral and enriched laterally rather than at cell-to-cell interface, which would suggest auxin efflux from cells into the environment. We speculate this might be the native function, as the morphologically simple filamentous structure of *Klebsormidium,* without polar growth or differentiated cell types during vegetative growth, provides little justification for the necessity of localized auxin gradients to maintain cell identity or trigger developmental changes as in three-dimensional land plant bodies. This could also be the case in other charophyte algae, where PIN homologs have been identified regardless of morphological complexity, even in unicellular representatives (Ju et al., 2015). The hypothetical purpose of the ancestral cell-to-environment auxin efflux might include quorum sensing or detoxification, as higher auxin concentration inhibits cell division in *Klebsormidium* (Ohtaka et al., 2017). When auxin became a significant agent in plant developmental regulation, PIN-mediated auxin transport would also become more complex, including the evolution of PIN polar localization to control its directionality. Intriguingly, the uniquely complex stoneworts *(Charophyceae)* might represent a case of convergent evolution of the recruitment of PINs to regulate an increasingly complex development: multiple *Chara* species show evidence of independent PIN radiation (Nishiyama et al., 2018), polar localization of PIN-like proteins (Zabka et al., 2017) and basipetal auxin transport (Boot et al., 2012), though the latter has not yet been connected to the native PINs. We conclude that PM-localized auxin transport is an ancient and conserved character within the PIN

family and emerged early in streptophyte evolution. The fascinating questions regarding the ancient and derived traits of PIN-mediated auxin transport, such as post-translational regulation by kinases and its utilization in separate branches of streptophytes will be addressed as more model organisms, especially from charophyte algae, become sufficiently established in research.

Methods

See the Supplementary Methods sections 'Plant material and chemicals' and 'Microscopy and statistics' concerning these issues, and for additional information concerning the sections below.

Molecular biology, transformation and reverse transcription

See Supplementary Methods for *KfPIN* and *KfPIN:GFP* cloning protocol and primer sequences. See Supplementary Figure 5 for RT-qPCR results. Total RNA was isolated from *K. nitens* biomass, *P. patens* fresh protonemal tissue, 2-week *A. thaliana* or 2-day BY-2 by Trizol (LifeTechnologies), purified with an RNeasy kit (Qiagen) and treated with DNAse (DNA-free Kit; Ambion). Iproof (BioRad) or M-MLV Reverse Transcriptase (Promega) were used for reverse transcription.

Phenotype analysis

Phenotype observation and evaluation in *P. patens* were performed as described (Viaene et al., 2014). Gravitropic root bending was observed 24 hours after turning 4-day *A. thaliana* plants by 90°; the process was repeated once after the first screen. Primary leaves of 9-day *A. thaliana* plants were cleared as described in Zhang et al., 2011 and categorized into "normal" (four distinct compartments of same or similar size) and "abnormal" vascular pattern (four compartments of markedly different sizes or >4 compartments initiated or finished). Root hair length was analyzed in 8-day *A. thaliana* plants. Cell parameters in BY-2 were measured in 3-day cells. Image analysis was performed in ImageJ.

Auxin transport and metabolism assays

Auxin accumulation and retention assays in BY-2 and *X. laevis* oocytes were performed as described (Petrasek et al., 2006 and Fastner et al., 2017). The absolute auxin export rates for three biological replicates in *X. laevis* oocytes were obtained as the slope value after linear regression of the three curves per variable (*Kf*PIN vs. *Kf*PIN+PID). PID refers to *A. thaliana* PINOID protein kinase (GenBank NM_129019). For negative control, oocytes were injected with water instead of mRNA. See Supplementary Methods for analysis of IAA content in the biomass and culture medium of *K. nitens*, and *P. patens* protonemata.

Immunostainings

*Kf*PIN in *A. thaliana* and *K. flaccidum* (strain UTEX #323) was immunolocalized as described (Paciorek et al., 2006) using the automated InsituPro VSi station slide module (Intavis). Before the procedure, *K. flaccidum* cells were fixed for 1 hour in 3.7% paraformaldehyde and placed on superfrost slides. The slides were then rinsed in pure methanol and subsequently in liquid nitrogen to improve surface adhesion of cells. See Supplementary Methods for antibodies.

References

Adamowski, M. & Friml, J. *Plant Cell* **27**, 20-32, doi:10.1105/tpc.114.134874 (2015).

Bennett, T. *Trends in Plant Science* **20**, 498-507, doi:10.1016/j.tplants.2015.05.005 (2015).

Boot, K. J. M., Libbenga, K. R., Hille, S. C., Offringa, R. & van Duijn, B. *Journal of Experimental Botany* **63**, 4213-4218, doi:10.1093/jxb/ers106 (2012).

Fastner, A., Absmanner, B. & Hammes, U. Z. Plant Hormones: Methods and Protocols, 3rd Edition Vol. 1497 Methods in Molecular Biology (eds J. KleineVehn & M. Sauer) 259-270 (Humana Press Inc, 2017).

Ganguly, A. *et al. Plant Physiology* **153**, 1046-1061, doi:10.1104/pp.110.156505 (2010).

Hori, K. *et al. Nature Communications* **5**, 9, doi:10.1038/ncomms4978 (2014).

Ju, C. L. *et al. Nature Plants* **1**, 7, doi:10.1038/nplants.2014.4 (2015).

Leliaert, F. *et al. Critical Reviews in Plant Sciences* **31**, 1-46, doi:10.1080/07352689.2011.615705 (2012).

Luschnig, C., Gaxiola, R. A., Grisafi, P. & Fink, G. R. *Genes & Development* **12**, 2175-2187, doi:10.1101/gad.12.14.2175 (1998).

Nishiyama, T. *et al. Cell* **174**, 448-+, doi:10.1016/j.cell.2018.06.033 (2018).

Muller, A. *et al. Embo Journal* **17**, 6903-6911, doi:10.1093/emboj/17.23.6903 (1998).

Ohtaka, K., Hori, K., Kanno, Y., Seo, M. & Ohta, H. *Plant Physiology* **174**, 1621-1632, doi:10.1104/pp.17.00274 (2017).

Paciorek, T., Sauer, M., Balla, J., Wisniewska, J. & Friml, J. *Nature Protocols* **1**, 104-107, doi:10.1038/nprot.2006.16 (2006).

Petrasek, J. *et al. Science* **312**, 914-918, doi:10.1126/science.1123542 (2006).

Petrasek, J., Zazimalova, E. *Biotechnology in Agriculture and Forestry* **58**, Nagata, T., Matsuoka, K., Inzé, D. (eds.), Springer-Verlag, Berlin Heidelberg, 107-115, doi: 10.1007/3-540-32674-X (2006).

Viaene, T. *et al. Current Biology* **24**, 2786-2791, doi:10.1016/j.cub.2014.09.056 (2014).

Xi, W. Y., Gong, X. M., Yang, Q. Y., Yu, H. & Liou, Y. C. *Nature Communications* **7**, 10,

199 doi:10.1038/ncomms10430 (2016).

200 Zhang, J. *et al. Developmental Cell* **20**, 855-866, doi:10.1016/j.devcel.2011.05.013 (2011).

201 Zabka, A. *et al. Plant Cell Reports* **35**, 1655-1669, doi:10.1007/s00299-016-1979-x (2016).

202 Zizkova, E. *et al. Annals of Botany* **119**, 151-166, doi:10.1093/aob/mcw194 (2017).

203 Zourelidou, M. *et al. Elife* **3**, 68, doi:10.7554/eLife.02860 (2014).

Acknowledgements

We thank E.D. Cooper and C.F. Delwiche for sharing the *Klebsormidium* transcriptome sequences before their publishing and valuable suggestions; Markéta Fílová and Roger Granbom for technical assistance. This work was financially supported by the Ministry of Education, Youth and Sports of Czech Republic under the projects CEITEC 2020 (LQ1601) [TN, MZ], MSM/LO1417 [RS, SV, JP]; the Czech Science Foundation, projects GA18-26981S [JF, MZ], GA17-17966Y [MZ], German Research Foundation (DFG) project HA3468/6-1 [UH], GA16-10948S [KM, PS, JP]; European Union's Horizon2020 program (ERC grant agreement n° 742985) [JF], and US NSF Award DEB-1036506. TN, MZ and EM acknowledge the core facility CELLIM of CEITEC supported by the Czech-BioImaging large RI project (LM2015062 funded by MEYS CR) and Core Facility Plant Sciences of CEITEC MU. KL and MK acknowledge the Knut and Alice Wallenberg Foundation (KAW), the Swedish Governmental Agency for Innovation Systems (VINNOVA), the Swedish Research Council (VR), and the Swedish Metabolomics Centre.

Author contributions

J.F., J.P. and R.S. conceptualized the project. R.S., E.M. and T.V. performed and analyzed most experiments. T.V. cloned most constructs. Y.Z. cloned the *PIN2::KfPIN:GFP* construct and produced and analyzed the *Arabidopsis* line. D.J. and U.H. provided data on *Xenopus* oocytes. M.Z. designed the anti-*Kf*PIN-specific antibody. M.K. analyzed auxin content in biomass and media. S.V. performed statistical analysis. M.Z., T.N., K.M., K.L., P.S., J.F. and J.P oversaw the experiments. R.S. wrote the manuscript and J.F. and J.P. oversaw writing.

Competing interests

The authors declare no competing interests.

Data availability

The underlying data of this study is available upon request.

Figures

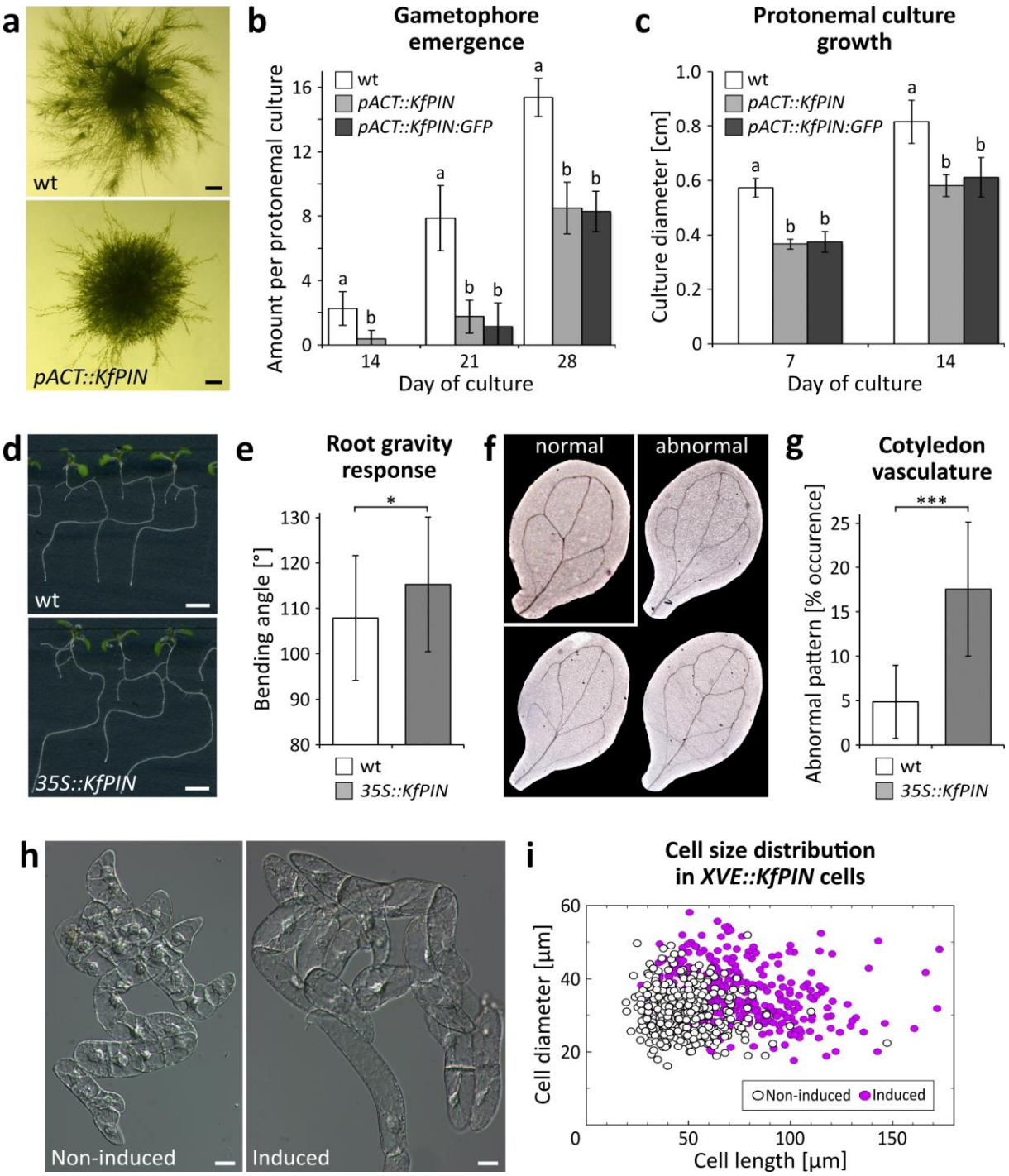

Figure 1 | *Kf*PIN expression in land plant models provokes phenotypes indicative of modulated auxin transport. a-c, *Physcomitrella patens.* **a**, Protonemal culture (2 weeks), wt vs. *pACT::KfPIN:GFP*. **b**, Quantification of protonemal culture growth rate, wt vs. *pACT::KfPIN* or *pACT::KfPIN:GFP*. Error bars SE, n=16. **c**, Quantification of gametophore emergence in protonemal

cultures, wt vs. *pACT::KfPIN* or *pACT::KfPIN:GFP*. Error bars SE, n=16. **d-g**, *Arabidopsis thaliana.* **d**, Gravitropic root bending in 8-day seedlings, wt vs. *35S::KfPIN*. **e**, Quantification of gravitropic root bending from 4 to 8 days old seedlings as in d. Average of 2 independent lines, error bars SE, n=916, P=0.005908 and 0.03071 for the first and second bend, respectively. **f**, "normal", most commonly occurring vein pattern vs. "abnormal", not commonly occurring vein pattern in 9-day plant primary leaves. **g**, Quantification of "normal" vs. "abnormal" leaf vascular pattern from **f**. Average of 2 independent lines, error bars SE, n=34, P=0.000 2337. **h**,**i**, *Nicotiana tabacum* BY-2 cells. **h**, Nomarski DIC of 3-day *XVE::KfPIN* cells, non-induced (left) vs. induced (right). **i**, Cell size (diameter vs. length) parameters from **h** (n=652). Scale bars 25 µm (**h**), 500 µm (**a**), 5 mm (**d**). Linear mixed-effect models were used for statistical analyses and the significance of their components was tested by likelihood ratio test. *P<0.05, ***P<0.001. "a" vs. "b" labels In **b** and **c**, the same model was used to determine the statistical significance between wt and transformant protonemal cultures in both culture size (labels "a" vs. "b" signify a statistical difference at P=0.05), and in differential growth rate (not shown).

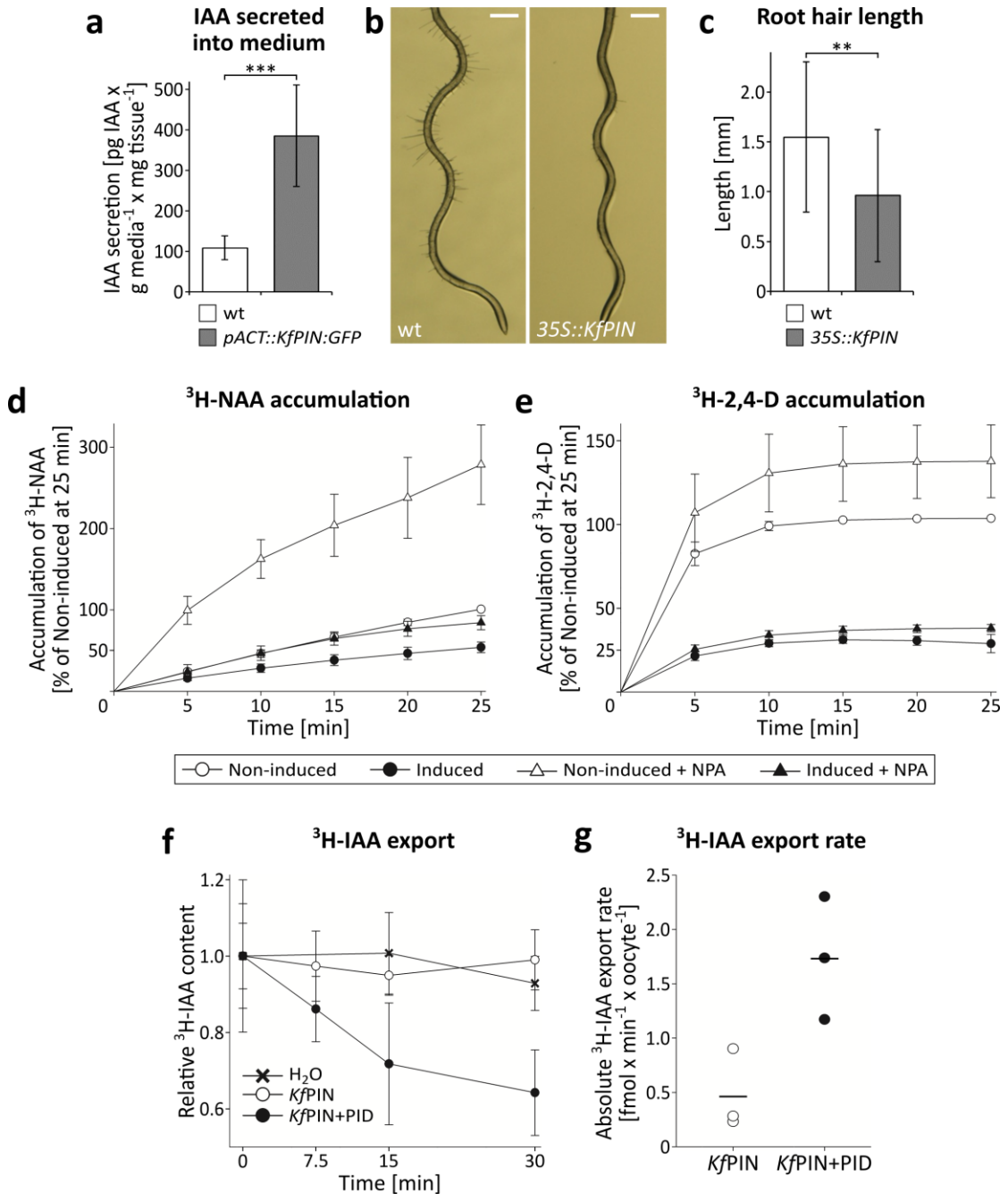

Figure 2 | *Kf*PIN auxin transport capacity. a, Quantification of auxin secretion into medium in *Physcomitrella patens* protonemal liquid culture, wt vs. *pACT::KfPIN:GFP*. Error bars SE, n=7, P=2.943×10^{-05}. **b**,**c**, Root hair length in 8-day *Arabidopsis thaliana*. **b**, wt plant vs. *35S:KfPIN* plant. **c**, Quantification of **b**. Average of 2 independent lines, error bars SE, n=240, P=0.00362. **d**,**e**, ^{3}H-labeled auxin accumulation in 1-day *XVE::KfPIN* cells of *Nicotiana tabacum* BY-2 with induced or non-induced expression. NPA (10 µM). **d**, ^{3}H-NAA, error bars SE, n=12. **e**, ^{3}H-2,4-D, error bars SE, n=12. **f**,**g**, ^{3}H-labeled auxin (IAA) retention over time in *Xenopus laevis* oocytes expressing either *Kf*PIN or

*Kf*PIN and PINOID (PID) kinase of *A. thaliana* (*Kf*PIN+PID). **f**, Representative experiment. One biological replicate, error bars SE, n=10. H_2O, oocytes injected with water instead of mRNA. **g**, Comparison of IAA transport rate between oocytes expressing either *Kf*PIN or *Kf*PIN+PID. Linear regression of 3 biological replicates, error bars SE. Scale bar 500 µm (**b**). Linear mixed-effect models were used for statistical analyses in **a** and **c** and the significance of their components was tested by likelihood ratio test. **P<0.01, ***P<0.001.

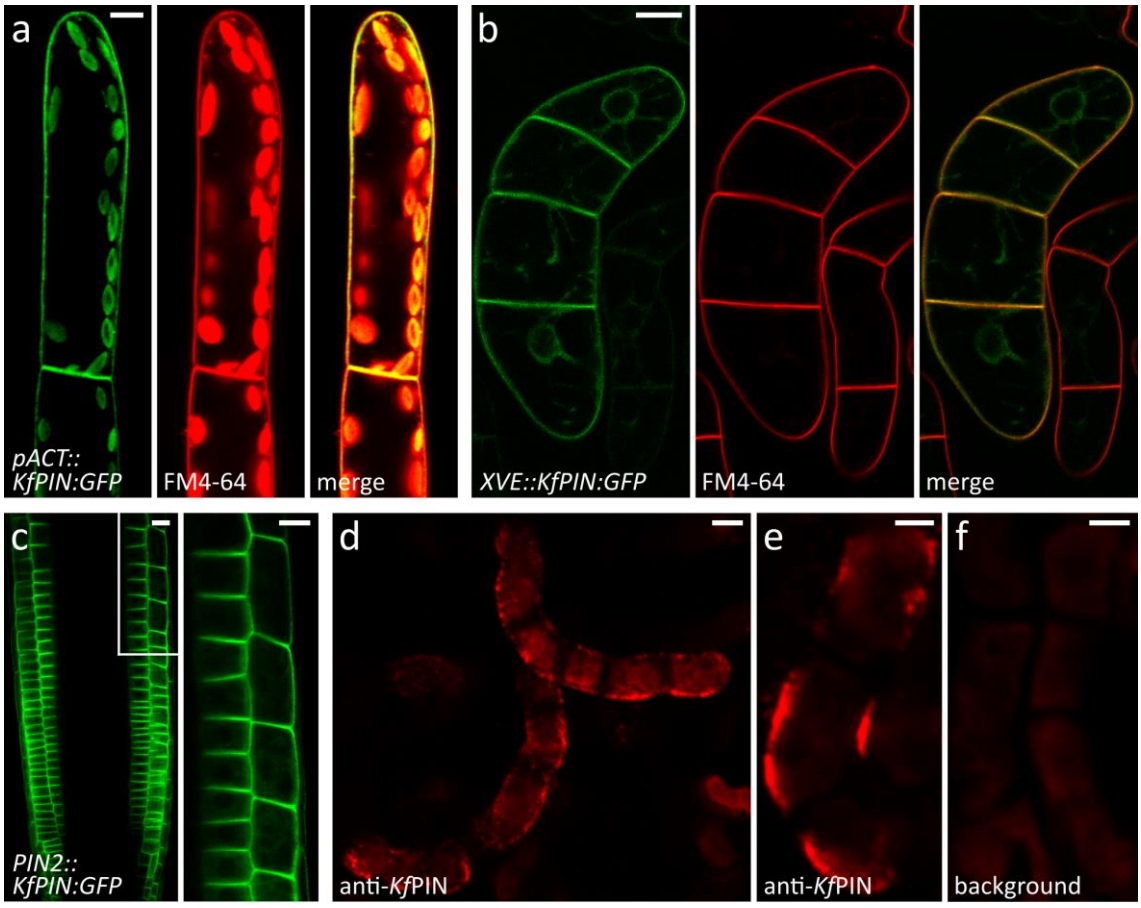

Figure 3 | *Kf*PIN subcellular localization. a-f, Confocal microscopy. **a**, *Physcomitrella patens* *pACT::KfPIN:GFP* protonema. GFP signal at the PM, FM 4-64 PM staining and merged image. Intracellular chloroplast autofluorescence is apparent in the green and red channels. **b**, *Nicotiana tabacum* BY-2 *XVE::KfPIN:GFP* cells, with induced expression. GFP signal at the PM and ER, FM 4-64 PM staining and merged image. **c**, *Arabidopsis thaliana PIN2::KfPIN:GFP* root. GFP signal predominantly at the PM. Whole root (left) and magnification of the marked area (right). **d-f**, *Klebsormidium flaccidum.* **d**,**e**, anti-*Kf*PIN indirect immunofluorescence, showing *Kf*PIN signal at the cell periphery. **f**, Control sample without primary antibodies showing background signal. Scale bars 20 µm (**b**), 10 µm (**c**), 5 µm (**a**,**d**,**f**), and 2.5 µm (**e**).

Supplementary Figures

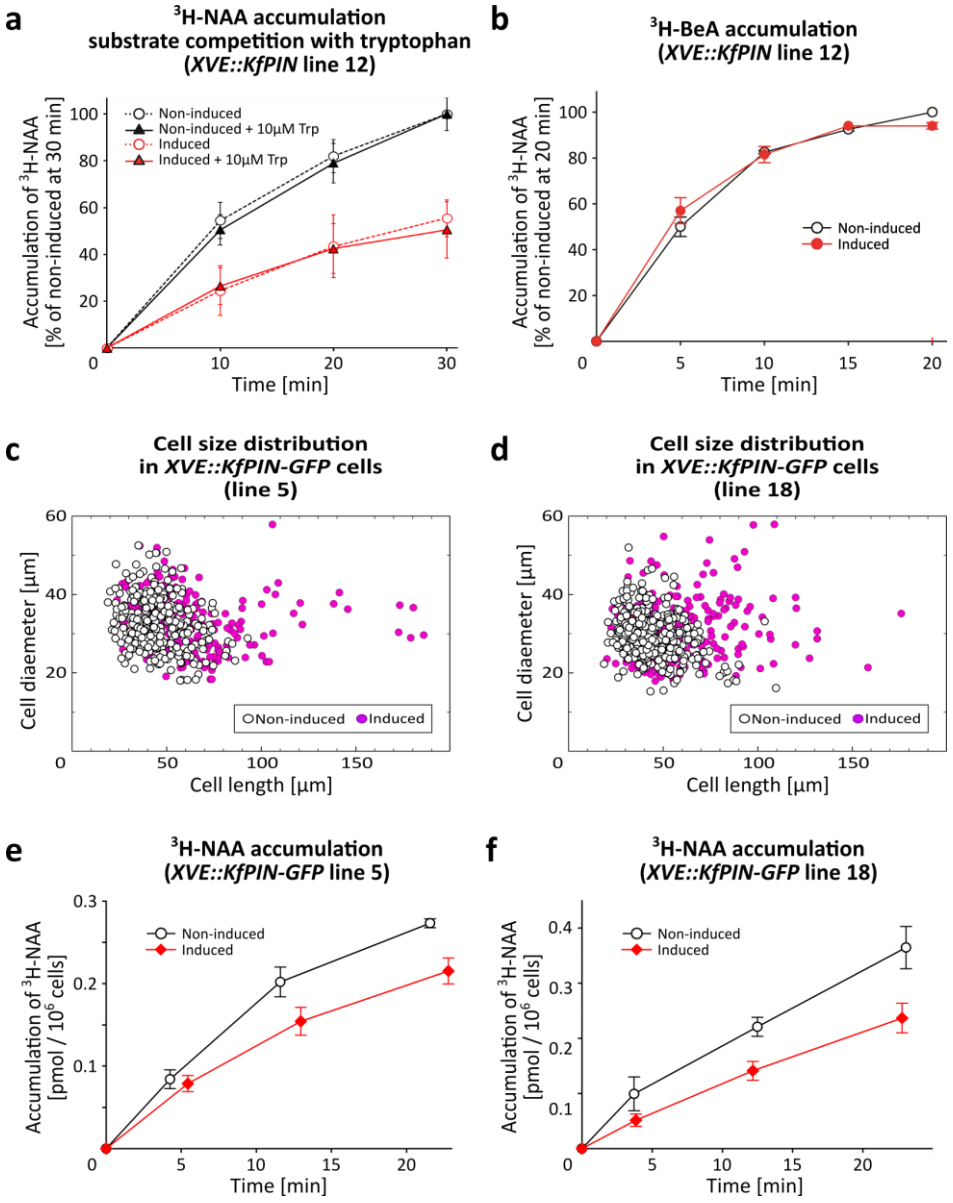

Supplementary Figure 1 | Auxin transport assays and phenotype analysis in *Nicotiana tabacum* BY-2 cells transformed with *XVE::KfPIN* and *XVE::KfPIN:GFP*. **a**, ^{3}H-NAA accumulation in induced and non-induced 1-day *XVE::KfPIN* cells showing no competition for uptake or efflux between ^{3}H-NAA and tryptophan, the latter being an auxin (indole-3-acetic acid) precursor and not an active auxin. Average from 2 repetitions, error bars SE (n=8). **b**, ^{3}H-BeA accumulation in induced and non-induced 1-day *XVE::KfPIN* cells, showing no export activity of *Kf*PIN for the inactive auxin analogue benzoic acid (BeA). Average from 2 repetitions, error bars SE (n=8). **c**,**d**, Cell size (diameter vs. length) parameters in two independent lines of 3-day *XVE::KfPIN:GFP* cells, each induced and

non-induced (**c**, n=510; **d**, n=570). **e**,**f**, ^{3}H-NAA accumulation in induced and non-induced 1-day *XVE::KfPIN:GFP* cells. Error bars SE (n=4). Lines 12 or 5, 18 represent independent transformations with *XVE::KfPIN or XVE::KfPIN:GFP*, respectively (see Supplementary Methods).

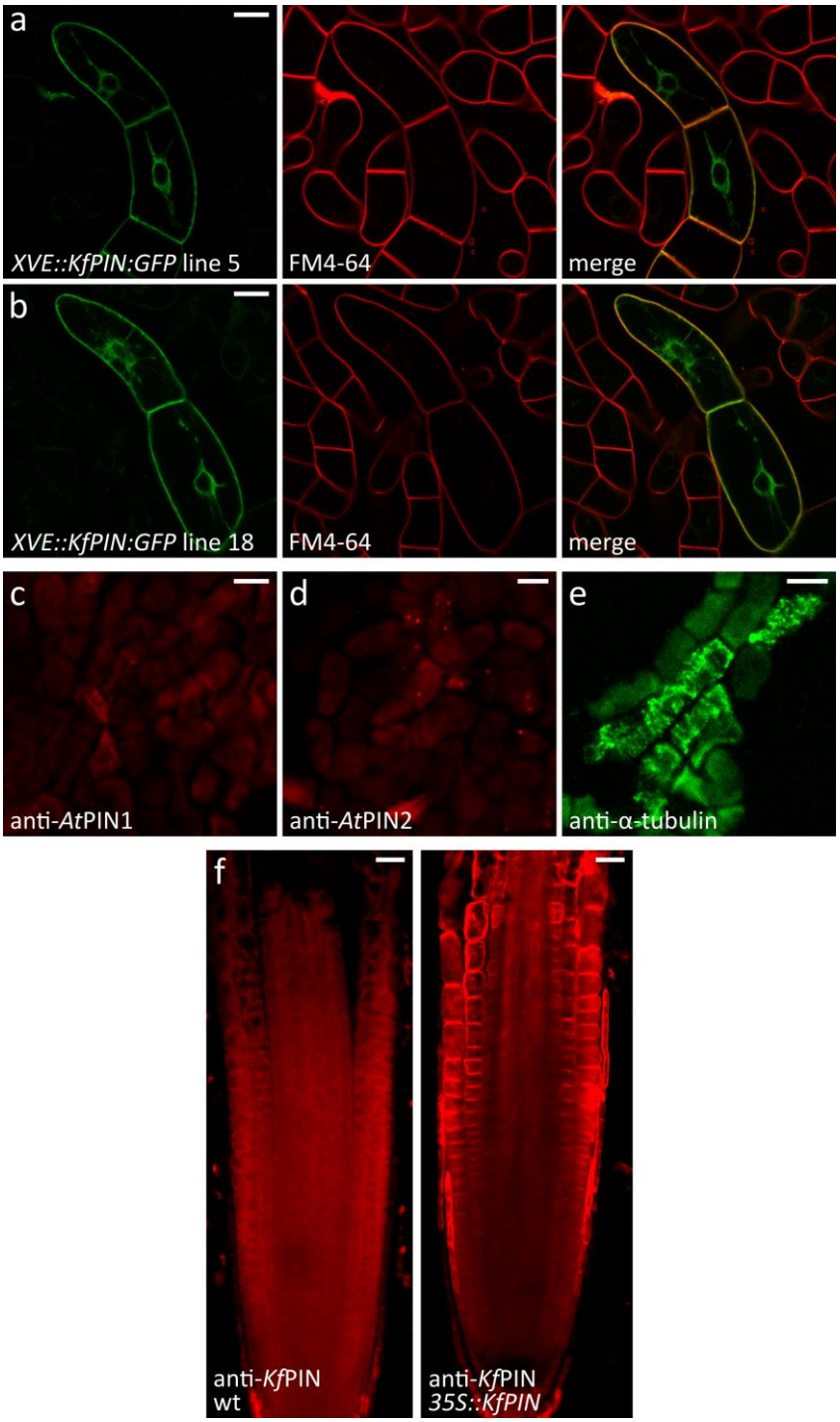

289

290 **Supplementary Figure 2 | Phenotypes of *Nicotiana tabacum* BY-2 cells with induced expression**
291 **in two independent *XVE::KfPIN:GFP* lines, controls for immunostaining of *Kf*PIN in**
292 ***Klebsormidium flaccidum* and immunostaining of *Kf*PIN in *35S::KfPIN Arabidopsis thaliana***
293 **roots. a-f**, Confocal microscopy. **a**,**b**, Two independent lines of 3-day *XVE::KfPIN:GFP* BY-2 cells
294 with induced expression. Left, GFP signal at the PM and ER showing cell expansion and elongation in
295 highly expressing cells. Middle, FM4-64 PM staining. Right, merged image. **c-e**, Indirect

immunofluorescence in *Klebsormidium flaccidum*. **c**, Immunostaining with anti-PIN1 antibody from *Arabidopsis thaliana* showing no signal. **d**, Immunostaining with anti-PIN2 antibody from *Arabidopsis thaliana* showing no signal. **e**, Immunostaining of α-tubulin showing microtubules in successfully stained cells. **f**, *Arabidopsis thaliana*, anti-*Kf*PIN indirect immunofluorescence. Immunostaining of *Kf*PIN in wt (left, background signal) vs. *35S::KfPIN* roots (right) showing PM localization. Scale bars 25 µm (**a**,**b**), 10 µm (**f**) and 5 µm (**c**,**d**,**e**).

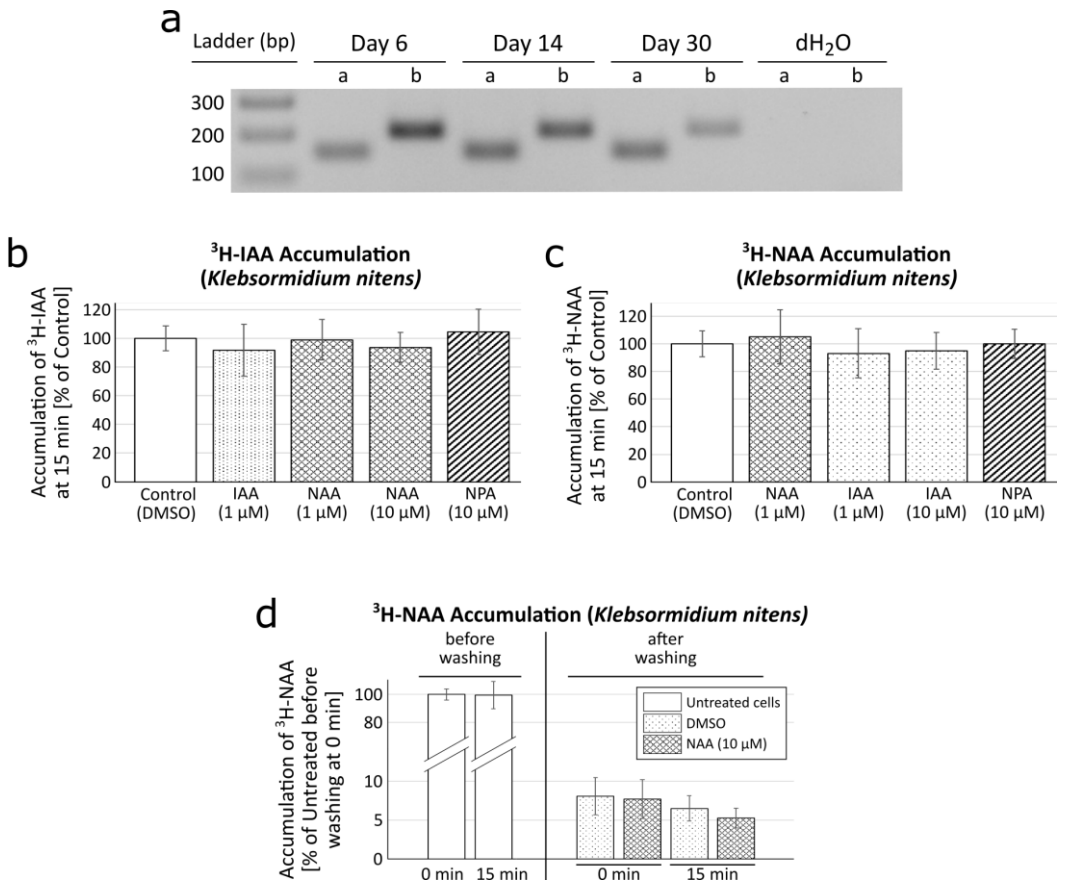

Supplementary Figure 3 | RT-PCR of *KfPIN* during a subculture interval and ^{3}H-labeled auxin transport assays in *Klebsormidium nitens*. **a**, RT-PCR targeted against the C-terminus of *KfPIN* coding sequence performed on samples from young (day 6), medium (day 14) and old (day 30) algal cultures showing transcription at all stages tested. Two independent sets of primers (a and b) were used. dH_2O, negative control. **b**,**c**, ^{3}H-labeled auxins accumulation in 6-day biomass. **b**, ^{3}H-labeled indole-3-acetic acid (^{3}H-IAA). **c**, ^{3}H-labeled 1-naphthaleneacetic acid (^{3}H-NAA). **d**, ^{3}H-NAA accumulation before and after washing out the ^{3}H-NAA-containing medium followed by re-suspension in clear medium. No significant increase in ^{3}H-labeled auxin accumulation indicative of substrate competition at auxin efflux or influx in media enriched with overabundant unlabelled auxin molecules was observed in **b-d**. Error bars SE (n=12, 3 biological repeats, 4 technical each).

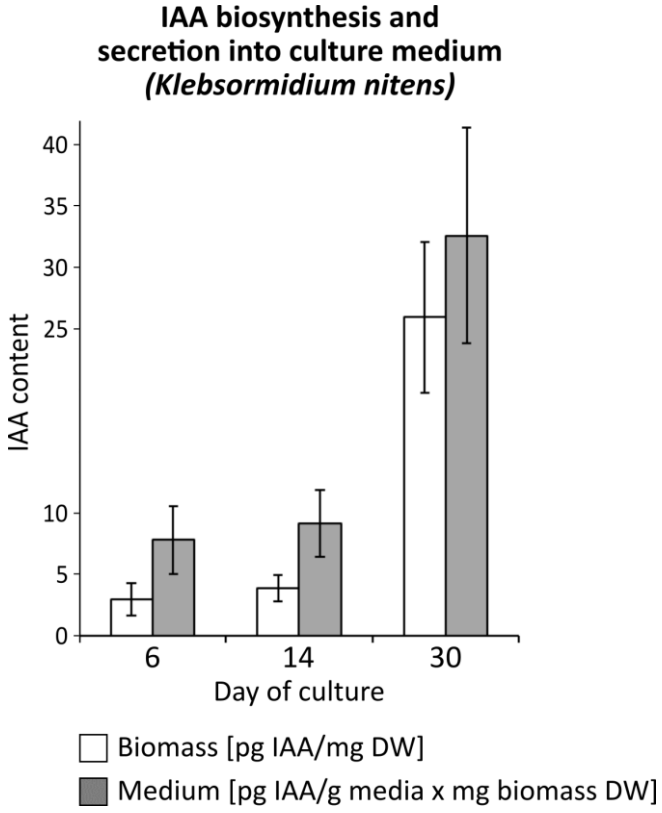

313

314 **Supplementary Figure 4 | Biosynthesis and secretion into culture medium of indole-3-acetic acid**

315 **(IAA) by *Klebsormidium nitens* during a subculture interval, sampled young (day 6), medium**

316 **(day 14) and old (day 30).** n=4, error bars SE. DW dry weight.

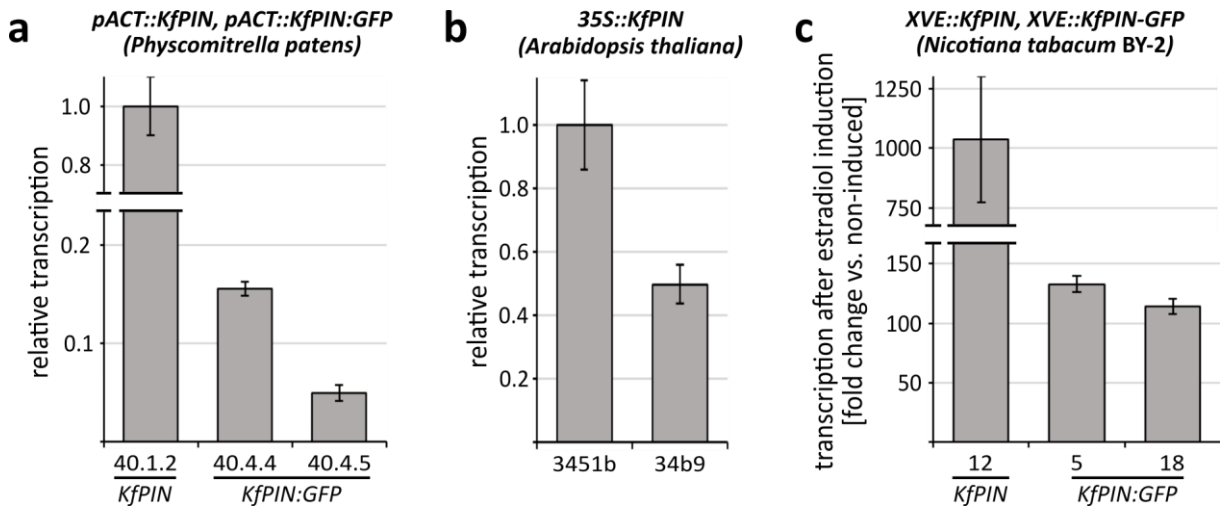

317

318 **Supplementary Figure 5 | RT-qPCR for *KfPIN* or *KfPIN:GFP* in transgenic land plant lines. a**,

319 *Physcomitrella patens* (*pACT::KfPIN* line 40.1.2 and *pACT::KfPIN:GFP*, lines 40.4.4 and 40.4.5). **b**,

320 *Arabidopsis thaliana* (*35S::KfPIN*, lines 3451b and 34b9). **c**, *Nicotiana tabacum* BY-2 (*XVE::KfPIN*,

321 line 12 and *XVE::KfPIN:GFP*, lines 5 and 18). Error bars SE.

Supplementary Methods

For references specific to the Supplementary Methods chapter, see the Supplementary methods references paragraph at its end.

Plant material and chemicals

Klebsormidium flaccidum strain UTEX #323 (Culture collection of Algae at University of Texas, Austin, USA) and *Klebsormidium nitens* strain NIES-2285 (National institute for environmental studies, Tsukuba, Japan) were cultured on solid (1.5% agar) C medium (Ichimura, 1971; see also NIES media list: http://mcc.nies.go.jp/02medium-e.html) at 30 µE light intensity at 16:8 light:dark regime. Initially, the work was performed on UTEX #323 (cloning of *KfPIN* coding sequence, immunolocalization). After the full genome sequence of NIES-2285 (then known as *Klebsormidium flaccidum*) has been published (Hori et al. 2014), we switched to this strain. However, NIES-2285 has later been re-classified as a different species, *Klebsormidium nitens*, hence the resulting state of two *Klebsormidium* species having been used in this study.

Physcomitrella patens ssp. *patens* strain Gransden protonemal tissue was cultured on cellophane-covered plates of BCD medium supplemented with 5 mM ammonium tartrate (BCD-AT) and 0.8% (w/v) agar (Thelander et al., 2007), with weekly sub-culture including tissue disruption in the Ultra-Turrax Tube Drive work system (IKA). For experiments with protonemal culture growth and gametophore initiation, the culture was grown on BCD medium plates (without ammonium tartrate, cellophane and weekly disruption) for a month. Growth conditions as follows: 24°C, 16-h light/8-h dark regime, light intensity 55 µmol m^{-2} s^{-1}.

Arabidopsis thaliana ecotype Columbia (Col-0) plants were grown vertically in Petri dishes with 0.5× Murashige and Skoog (MS) medium containing 1% (w/v) sucrose and 0.8% (w/v) agar, pH 5.9. Growth conditions as follows: 18°C under long day light regime (light intensity: 250 µmol per m^{-2} s^{-1}).

Nicotiana tabacum Bright Yellow-2 (BY-2) was cultured as in Petrasek et al., 2003.

Radiochemicals used were as follows: [^{3}H]-1-naphthaleneacetic acid (20 Ci $mmol^{-1}$), [$^{2,3,5\text{-}3}$H]-benzoic acid (60 Ci $mmol^{-1}$) (both American Radiolabeled Chemicals) and [^{3}H]-2,4-

dichlorophenoxyacetic acid (19.6 Ci $mmol^{-1}$) (Isotope Laboratory of the Institute of Experimental Botany, ASCR, Prague, Czech Republic).

Molecular biology, transformation and reverse transcription

All listed primer sequences are in 5' to 3' direction.

Full-length *KfPIN* coding sequence was obtained from the at the time unpublished transcriptome database of E. D. Cooper and C. F. Delwiche, performed on *Klebsormidium flaccidum* strain UTEX #321 (published in Ju et al., 2015). Because the strain was temporarily unavailable at the beginning of this study, we amplified the homologous *Kf*PIN coding sequence from *K. flaccidum* strain UTEX #323 (GenBank KJ466099.2), and this is the *Kf*PIN sequence investigated in this manuscript.

The *Kf*PIN coding sequence was amplified from K. flaccidum UTEX #323 using Phusion High-Fidelity DNA Polymerase (ThermoFisher) and cloned into the Gateway donor vector pDONR221 with primers GGGGACAAGTTTGTACAAAAAAGCAGGCTCCATGGCATCCGGCGGCCATGGCAGCATCAC and GGGGACCACTTTGTACAAGAAAGCTGGGTCTCAGAAGTGTTCCAGCGCGAC. eGFP gene (no stop codon) was inserted behind 270th amino acid (corresponding to the middle of the predicted protein hydrophilic loop) by overlapping PCR, using primers TCCTCGCCCTTGCTCACCATCTCCGCAGGATTACCTAGAC, GCATGGACGAGCTGTACAAGGAGTTCCGGATACAGATTAA, GTCTAGGTAATCCTGCGGAGATGGTGAGCAAGGGCGAGGA and TTAATCTGTATCCGGAACTCCTTGTACAGCTCGTCCATGC, and cloned into pDONR221 with the same primers listed above for the untagged sequence. The *Arabidopsis thaliana* PIN2 promoter (1.4 kb upstream of start codon) was cloned into the Gateway donor vector pPONRP4P1r with primers TATAGAAAAGTTGTAAATAGTTTCATCCTGTTTTATCAGGCTACATTCAC and TTTGTACAAACTTGATTTGATTTACTTTTTCCGGCGAGAGAGAGAAGAAG.

To generate the *pACT::KfPIN* and *pACT:KfPIN:GFP* constructs for *Physcomitrella patens,* the *KfPIN* or *KfPIN:GFP* gene constructs in pDONR221 were, each separately, fused with actin promoter from rice (*pACT*) via intermediary vectors pXb2-m43GW and pDONRP4P3 and cloned into the

destination vector pL5-m34GW7-L3 (see Viaene et al., 2014). Transformation via PEG (polyethylene glycol) was performed as described (Nishiyama et al., 2000), transformants were selected on plates supplemented with G418 (50 µg/ml).

To generate the *35S::KfPIN* construct for *Arabidopsis thaliana*, the *KfPIN* gene construct in pDONR221was cloned into the destination vector pB7WG2. To generate the *PIN2::KfPIN:GFP* construct for *A. thaliana*, the *KfPIN:GFP* gene construct in pDONR221 was fused with PIN2 promoter in pPONRP4P1r, into the destination vector pB7m24GW.3. *A. thaliana* was transformed via floral dip, using *Agrobacterium tumefaciens* strain C58C1. *35S::KfPIN* transgenic plants were selected on plates supplemented with BASTA (15 mg/l). *PIN2::KfPIN:GFP* plants were screened simply by observing fluorescence in T1 generation and propagated into T2 generation. The images in Figure 3c represent one selected *PIN2:KfPIN:GFP* fluorescent line from T2 generation.

To generate the *XVE::KfPIN* and *XVE::KfPIN:GFP* estradiol-inducible expression constructs for *Nicotiana tabacum* BY-2 cells, the *KfPIN* or *KfPIN:GFP* gene constructs in pDONR221 were, each separately, cloned into the destination vector pMDC7 (Curtis and Grossniklaus, 2003). Transformation was performed as described (Petrasek et al., 2003) using *Agrobacterium tumefaciens* strain GV2260. Transformed calli were obtained on selection plates supplemented with hygromycin (40 mg/l; transgene selection) and cefatoxime (300 mg/l; bactericide). Expression was induced by 1.5 µM estradiol.

Quantitative real-time PCR was performed using GoTaq qPCR Master Mix (Promega) at 58°C T_a on LighCycler480 instrument (Roche). For *Nicotiana tabacum* BY-2, PCR efficiency was estimated using serial dilution of template cDNA, using the Tobacco *EF1a* gene (GenBank AF120093) as reference for relative quantification, and relative transcription was calculated using equation:

$$\text{ratio} = \frac{\text{eff}_{\text{ref}}^{\text{CP}_{\text{ref}}}}{\text{eff}_{\text{target}}^{\text{CP}_{\text{target}}}}$$

Where eff_{ref} and $\text{eff}_{\text{target}}$ stand for qPCR efficiency of the reference gene and the target gene, respectively, and CP_{ref} and $\text{CP}_{\text{target}}$ stand for crossing point of the reference gene and the target gene, respectively. For RT-qPCR in *Nicotiana tabacum* BY-2, the reference gene (Elongation factor *EF1a*,

GenBank AF120093) primers were TGAGATGCACCACGAAGCTC and CCAACATTGTCACCAGGAAGTG and the primers for *KfPIN* gene constructs GCCTGCGATAATGGGAGTAA and AAATGTGATGCTGGTGCTCA. For RT-qPCR in *Physcomitrella patens* and *Arabidopsis thaliana*, the primers for *KfPIN* gene constructs were AGAGTTCGCCCTCACAGAAT and GCTGGAAGGACTATCTTGGC. *Physcomitrella patens* reference gene (Elongation factor 1-alpha, GenBank XM_024541223) primers were AATCATACATTTCACCTCGCC and GATCAGTGGGTAGAAGTGAC. *Arabidopsis thaliana* reference gene (Eukaryotic translation initiation factor 4A1, GenBank NM_001338093) primers were ACGGAGACATGGACCAGAAC and GCTGAGTTGGGAGATCGAAG. For RT-PCR of the native homolog of *KfPIN* in *Klebsormidium nitens*, two sets of primers were designed targeting the conserved regions between the PIN homologs of *K. flaccidum* (UTEX #323) and *K. nitens* (NIES-2285). The first primer set was labelled as "a" (CTGGCATCAACCGCTTTGTG and TAGACCGCCAGCACAACAAG), the second as "b" (CACCCTTATCGTTGGCGTGC and TTTCACCTCTGCCCCTGC) and their products from *K. nitens* cDNA were amplified using Phusion High-Fidelity DNA Polymerase (ThermoFisher), cloned into pGEM-T Easy plasmid (Promega) and verified by sequencing.

Auxin transport and metabolism assays

Radiochemical solutions were diluted 5x in 99.8% EtOH, quality grade for UV (Lach-Ner), and added to final concentration of 2 nM during experiments. 1-day *Nicotiana tabacum* BY-2 (induced upon inoculation) was used to prevent the auxin starvation phenotype build-up in later culture stages. The accumulation experiments on *Klebsormidium nitens* (strain NIES-2285) were performed on 6-day biomass suspended in fresh culture medium (C medium without TRIS, pH 5.5; 100 mg biomass fresh weight/10 ml), each sample equaled 1 ml of suspension with four samples per time point. Radioactivity within samples was measured on a Tri-Carb 4910TR Liquid Scintillation Analyzer (PerkinElmer).

For analysis of auxin (IAA) biosynthesis and excretion in the biomass of a 6-week *K. nitens* (strain NIES-2285) was suspended in fresh liquid culture medium (20 mg/ml) and inoculated onto fresh solid

culture media in Erlenmeyer flasks as follows: 450 µl (i.e. 9 mg) per 20 ml medium in a 50-ml flask, or 900 µl per 40 ml in a 100-ml flask for the "day 6" samples to achieve higher biomass amounts at that sampling point. The biomass samples were scraped off medium into tubes, frozen in liquid nitrogen and lyophilized before analyses. For analyses of auxin (IAA) content in *Physcomitrella patens* protonemal biomass and medium over time, 1/5 of total biomass grown on plate for 11 days was added into 9 ml of liquid BCD medium in a 15-ml falcon tube and cultured horizontally under mild shaking in standard growth conditions. The tube cap was briefly loosed 1-2 times a day to allow gas exchange. After 4 days, aliquots of 1 ml medium and ca. 20 mg biomass were collected and flash-frozen in liquid N_2. The biomass and medium before inoculation and before sampling were weighed, as were the biomass and medium samples. The samples of both *K. nitens* and *P. patens* were processed and analyzed as follows: frozen samples were homogenized by bead mill (MixerMill, Retsch GmbH) and extracted in 1 ml of 50mM sodium phosphate buffer containing 1 % of sodium diethyldithiocarbamate and a mixture of $^{13}C_6$ or deuterium labelled internal standards. After pH adjustment to 2.7 by 1M HCl, a solid-phase extraction was performed using Oasis HLB columns (30mg 1cc, Waters Inc.). Mass spectrometry analysis and quantification was performed by LC-MS/MS system comprising of 1290 Infinity Binary LC System coupled to 6490 Triple Quad LC/MS System with Jet Stream and Dual Ion Funnel technologies (Agilent Technologies). See Novak et al.,2012 for more details.

Immunostainings

anti-*Kf*PIN (1:250; Rabbit) specific polyclonal antibody was raised against recombinant proteins corresponding to amino acid 171-355 representing KfPIN hydrophilic loop. Peptides were expressed from vector pLATE31 and purified as C-terminally 6× His-tagged versions.

Commercial Anti-tubulin primary antibody (ThermoFisher Scientific MA1-25063), Mouse, was used 1:500.

The newly raised anti-PIN primary antibodies against PIN1 and PIN2 of *Arabidopsis thaliana* were used for the first time in this publication, but are based on previously chosen protein fragments: Anti-**PIN1** (1:500); Rabbit; specific polyclonal antibody raised against PIN1 fragment encompassing amino

456 acids 288-452, previously used in Paciorek et al., 2005. Anti-**PIN2** (1:500); Rabbit; specific
457 polyclonal antibody raised against PIN2 fragment encompassing amino acids 189–477, previously
458 used in Abas et al., 2006. Indicated peptides were expressed in vector pDEST17 and purified as N-
459 terminally 6×His-tagged versions. The anti-*Kf*PIN, anti-PIN1 and anti-PIN2 sera were generated by
460 Moravian Biotechnology Ltd.
461 The secondary antibodies used were as follows: Cy3-conjugated Sheep anti-Rabbit IgG (Sigma
462 Aldrich; C2306), used 1:600. Alexa Fluor 488 Goat anti-Mouse IgG (ThermoFisher Scientific
463 A11001), used 1:600.

464 **Microscopy and statistics**

465 DIC microscopy was performed on Nikon Eclipse E600 (Nikon Japan) and Leica DMI4000B inverted
466 microscope. Confocal microscopy was performed using Zeiss LSM710 and Zeiss LSM880. 5 μM FM
467 4-64 dye (ThermoFisher Scientific) for plasma membrane staining was applied for 5 min on ice and
468 the samples observed immediately.
469 Statistical evaluation was performed using R software package (R Core Team, 2013). Data were
470 fitted by linear mixed-effect models (using 'lmer' function from package 'lmer4'), i.e. with fixed
471 effects (e.g. genotype) and random effects (biological replications). Data representing gametophore
472 emergence and cotyledon vasculature were fitted by generalized mixed-effects models with binomial
473 and Poisson distributions, respectively (function 'glmer' from package 'lme4'). Significances of
474 individual effects were determined by likelihood ratio test comparison of full and dropped models
475 using 'anova' function (Bates et al., 2015). Significance within multiple-level parameters was
476 evaluated by Tukey multiple comparison ('glht' function from package 'multcomp').
477 A single transgenic line was considered a biological repetition; any number of the same
478 experiments on a single line were considered technical repetitions.

479 **Transgenic lines**

480 Transgenic lines produced for model organisms used in this study as follows. See Supplementary
481 Figure 5 for the matching RT-qPCR results.
482 *Physcomitrella patens* lines: *pACT::KfPIN* **40.1.2**, *pACT::KfPIN:GFP* **40.4.5**.

Arabidopsis thaliana lines: *35S::KfPIN* **3451b**, *35S::KfPIN* **34b9**. *PIN2::KfPIN:GFP* (one line, no specific label)

Nicotiana tabacum BY-2 lines: *XVE::KfPIN* **12**, *XVE::KfPIN:GFP* line **5**, *XVE::KfPIN:GFP* line **18**.

Representation of all lines in Figures and Supplementary Figures as follows.

Figure 1: **a)** 40.4.5. **b,c)** 40.1.2 and 40.4.5. **d)** 3451b. **e,f,g)** 3451b and 34b9. **h,i)** 12

Figure 2: **a)** 40.4.5. **b)** 34b9. **c)** 3451b and 34b9. **d,e)** 12.

Figure 3: **a)** 40.4.4. **b)** 18.

Supplementary Figure 1: **a,b)** 12. **c,e,)** 5. **d,f)** 18.

Supplementary Figure 2: **a)** 5. **b)** 18. **f-right)** 3451b.

Supplementary methods references

Abas, L. *et al. Nature Cell Biology* **8**, 249-256, doi:10.1038/ncb1369 (2006).

Bates, D., Machler, M., Bolker, B. M. & Walker, S. C. *Journal of Statistical Software* **67**, 1-48 (2015).

Curtis, M. D. & Grossniklaus, U. *Plant Physiology* **133**, 462-469, doi:10.1104/pp.103.027979 (2003).

Ichimura, T. Proceedings of the Seventh International Seaweed Symposium, University of Tokyo Press, Tokyo, 208-214 (1971).

Nishiyama, T., Hiwatashi, Y., Sakakibara, K., Kato, M. & Hasebe, M. *DNA Research* **7**, 9-17, doi:10.1093/dnares/7.1.9 (2000).

Novak, O. *et al. Plant Journal* **72**, 523-536, doi:10.1111/j.1365-313X.2012.05085.x (2012).

Paciorek, T. *et al. Nature* **435**, 1251-1256, doi:10.1038/nature03633 (2005).

Petrasek, J. et al. Plant Physiology **131**, 254-263, doi:10.1104/pp.012740 (2003).

R CORE TEAM. R. Vienna, Austria: R Foundation for Statistical Computing (2013).

Thelander, M. *et al.* Plant Molecular Biology 64, 559-573, doi:10.1007/s11103-007-9176-5 (2007).